On short cracks that depart from elastoplastic notch tips

Verônica Miquelin Machado, Jaime Tupiassú Pinho de Castro, Marco Antonio Meggiolaro
Pontifical Catholic University of Rio de Janeiro, PUC-Rio, R. Marquês de São Vicente 225, Rio de Janeiro, 22451-900, Brazil
ferreirase@hotmail.com, jtcastro@puc-rio.br, meggi@puc-rio.br

ABSTRACT. The behavior of short cracks that depart from elastoplastic notch tips is modeled to estimate the stresses required to initiate and to propagate cracks in notched structural components, and to evaluate the size of tolerable crack-like defects under general loading conditions. This analysis can model both fatigue and environmentally assisted cracking problems; can evaluate notch sensitivity in both cases; and can as well be used to establish design or acceptance criteria for tolerable non-propagating crack-like defects in such cases. The growth of short cracks is assumed driven by the applied stresses and by the stress gradient ahead the notch tip, and supported by the material resistances to crack initiation and to long crack propagation by fatigue or EAC. In the elastoplastic case, the stress gradient ahead of the notch tip is quantified by a *J*-field to consider the short crack behavior. The tolerable short crack predictions made by this model are evaluated by suitable fatigue and EAC tests of notched specimens specially designed to start non-propagating cracks from the notch tips, both under elastic and elastoplastic conditions.

KEYWORDS. Short cracks; Notch sensitivity; Fatigue cracking; Environmentally assisted cracking; Elastoplastic behavior; J-integral.

Citation: Machado, V.M., Castro, J.T.P., Meggiolaro, M.A., On short cracks that depart from elastoplastic notch tips, Frattura ed Integrità Strutturale, 41 (2017) 242-250.

Received: 28.02.2017
Accepted: 03.05.2017
Published: 01.07.2017

INTRODUCTION

It is well-known that abrupt geometric transitions (like holes, slots, grooves, keyways, shoulders, corners, threads, weld fillets, reinforcements, etc.), generically called notches, perturb the local stress field around their borders. In particular, notches induce a localized stress concentration factor $K_t = \sigma_{max}/\sigma_n$ under linear elastic (LE) loading conditions, where σ_{max} is the maximum stress around the notch borders and σ_n is the nominal stress that would act there if the notch did not disturb the stress field in its vicinity. It is also well-known that notch-induced effects under fatigue load conditions can be smaller than it would be predicted from $K_t \cdot \sigma_n$, in particular if K_t is high. If this was not so, small sharp scratches would be able to ruin any structural component subjected to fatigue loads. Therefore, notch effects in fatigue are often quantified in practical applications by $K_f = 1 + q \cdot (K_t - 1)$, where $0 \le q \le 1$ is the notch sensitivity factor.

For design purposes, q-values are traditionally estimated by fitting semi-empirical models to data from fatigue tests of notched components.
However, q has long been associated to non-propagating short cracks that start at the notch tips but stop after growing for a small distance [1-3]. So, q-values can also be analytically modeled by studying the behavior of those short fatigue cracks. In particular, the model proposed in [4] estimates q-values for fatigue loading conditions using sound mechanical principles and well-defined mechanical properties, without the need for any additional data-fitting parameter. Moreover, it allows the notch sensitivity concept to be extended to environmentally-assisted cracking (EAC) problems as well, and its predictions have been validated under liquid metal embrittlement conditions by testing notched Al samples in a Ga environment [5], as well as under hydrogen embrittlement conditions by testing similar steel samples in aqueous H_2S environments [6]. This versatile notch sensitivity model is extended in this work to deal with elastoplastic (EP) problems using J-integral techniques properly adapted to consider the short crack behavior near the notch tips.

INFLUENCE OF SHORT CRACKS IN THE FATIGUE LIMIT OF NOTCHED STRUCTURAL COMPONENTS

Fatigue cracks are very sensitive to local load conditions, so they usually initiate at notch tips due to the stress concentration effects induced by the notch. A similar behavior occurs under EAC conditions as well. However, it is less well-known that short cracks initiated at notch tips can stop to grow if the stress gradient ahead of the tip is steep enough. In fact, albeit such non-propagating cracks induce damage, they can be tolerated whenever the loading conditions cannot induce the higher local stresses needed to restart their growing process. This apparently odd behavior can be easily explained by the competition between the opposing effects of the decreasing stress σ ahead of the crack tip (due to the stress gradient that acts there) and of the increasing crack size a on its stress intensity factor (SIF) $K \approx \sigma \cdot \sqrt{(\pi \cdot a)}$, which can be seen as the crack driving force under LE conditions. To make the crack size dependent SIF compatible with a fatigue limit when $a \to 0$, El-Haddad, Topper, and Smith (ETS) redefined the SIF range acting in a Griffith plate by [7-8]

$$\Delta K = \Delta\sigma \cdot \sqrt{\pi (a + a_0)} \tag{1}$$

where $a_0 = (1/\pi)(\Delta K_0/\Delta S_0)$ is the short crack characteristic size, ΔK_{th0} is the long fatigue crack growth threshold and ΔS_{L0} is the fatigue limit at $R = \sigma_{min}/\sigma_{max} = 0$, both well-defined material properties that can be measured by standard procedures. This simple but clever trick reproduces the correct limits $\Delta\sigma(a \to 0) \to \Delta S_0$ for very short cracks and $\Delta K(a >> a_0) \to \Delta K_{th0}$ for long cracks, as well as the data trend in a Kitagawa-Takahashi $\Delta\sigma \times a$ diagram by predicting that cracks do not grow whenever $\Delta\sigma \le \Delta K_{th0}/\sqrt{\pi}(a + a_0)$ [3-8].
Since cracks that depart from notches are driven by the local stress field around their tips, if the geometry factors $g(a/w)$ used in their SIFs include K_t effects, as usual, it is convenient to split into two parts, $g(a/w) = \eta \cdot \varphi(a)$. In this way $\varphi(a)$ quantifies stress gradient effects near the notch and tends towards K_t at its tip, $\varphi(a \to 0) \to K_t$; whereas η accounts for other effects that affect the SIF, like the free surface, for instance. Moreover, since the SIF is a crack driving force, it should be material-independent. So, the a_0 effect on the short-crack behavior should be used to modify the fatigue crack growth (FCG) threshold instead of ΔK, making it a function of the crack size and of the fatigue limits, a trick that is quite convenient for operational purposes. In this way, the FCG threshold for pulsating loads $\Delta K_{th}(a, R = 0) = \Delta K_{th0}(a)$ is given by:

$$\frac{\Delta K_{th_0}(a)}{\Delta K_{th_0}} = \frac{\Delta\sigma\sqrt{\pi a} \cdot g(a/w)}{\Delta\sigma\sqrt{\pi(a + a_0)} \cdot g(a/w)} = \sqrt{\frac{a}{a + a_0}} \Rightarrow \Delta K_{th_0}(a) = \Delta K_{th_0}\left[1 + (a_0/a)\right]^{-1/2} \tag{2}$$

However, since FCG depends both on ΔK and K_{max}, Eq. (2) should be modified to consider the K_{max} (or the R-ratio) effect on the short crack behavior. Moreover, it can also be seen as just one of the models that obey the long-crack and the microcrack limits, so it can include a data fitting parameter γ [3]. So, if $\Delta K_{thR} \equiv \Delta K_{th}(a >> a_R, R)$ is the FCG threshold for long cracks and $\Delta S_{LR} \equiv \Delta S_L(R)$ is the fatigue limit of the material, both measured (or estimated) at the desired R-ratio, then:

$$\Delta K_{th_R}(a) = \Delta K_{th_R} \cdot \left[1 + (a_R/a)^{\gamma/2}\right]^{-1/\gamma}, \text{ where } a_R = (1/\pi) \cdot \left[\Delta K_{\mathrm{th_R}} \Big/ \left(\eta \cdot \Delta S_{\mathrm{L_R}}\right)\right]^2 \tag{3}$$

Equation (3) reproduces the ETS model when $\gamma = 2$, and the bi-linear limits in Kitagawa-Takahashi diagrams as well, see [3] for details. But much more important, it can be used to answer questions that are quite important in practical applications. For example, this model can be used to check if it is possible to replace a central circular hole with diameter $d = 20mm$ by an elliptical one with axes $2b = 20mm$ (perpendicular to $\Delta\sigma_n$) and $2c = 2mm$, in a large notched steel plate with tensile strength $S_U = 600MPa$, $S_L = 200MPa$, and $\Delta K_{th0} = 9MPa\sqrt{m}$, which works under a constant fatigue load $\Delta\sigma_n = 100MPa$ and $R = -1$.

Neglecting buckling to start with, using classic *SN* procedures studied in most machine design textbooks [9-11], the circular hole would have a safety factor $\phi_F = S_L/K_f\sigma_n = 200/150 \cong 1.33$ against fatigue crack initiation, since due to its large radius it has $K_f \cong K_t = 3$. However, since the elliptical hole tip radius is $\rho = c^2/b = 0.1mm \Rightarrow K_t = 1 + 2b/c = 21 \Rightarrow K_f = 1 + q\cdot(K_t - 1) = 7.33$ (according to Peterson's estimate, $q = (1 + \alpha/\rho)^{-1} = [1 + 0.185\cdot(700/600)/0.1]^{-1} \cong 0.32$ [12]), it would fail by classic *SN* procedures. Indeed, it would work under a stress amplitude $\sigma_a = K_f\cdot\sigma_n \cong 367MPa > S_L$. However, since this K_f value is larger than the $K_f < 4$ typically obtained from notched coupons fatigue data [3], it is worthwhile to reevaluate this prediction.

Assuming e.g. $\Delta K_{th0}(a) = \Delta K_{th0}/[1 + (a_0/a)]^{-0.5}$ (by ETS), the steel fatigue limit $S_L = S_U/2$ (as usual), $\Delta S_{L0} = S_U/1.5$ (by Goodman) and $a_0 = (1/\pi)(\Delta K_{th0}/\eta\Delta S_{L0})^2 = (1/\pi)(1.5\Delta K_{th0}/1.12\cdot S_U)^2 \cong 0.13mm$, then the SIF ranges $\Delta K_I(a)$ estimated for the two holes by the procedures developed in [4] are compared to the short-crack threshold $\Delta K_{th0}(a)$ in Fig. 1. Notice that the curve crossings in this figure define crack arrest, so the largest tolerable crack sizes. Hence, this model predicts that both the circular and the elliptical holes could support the nominal load range $\Delta\sigma_n$ without failing by fatigue.

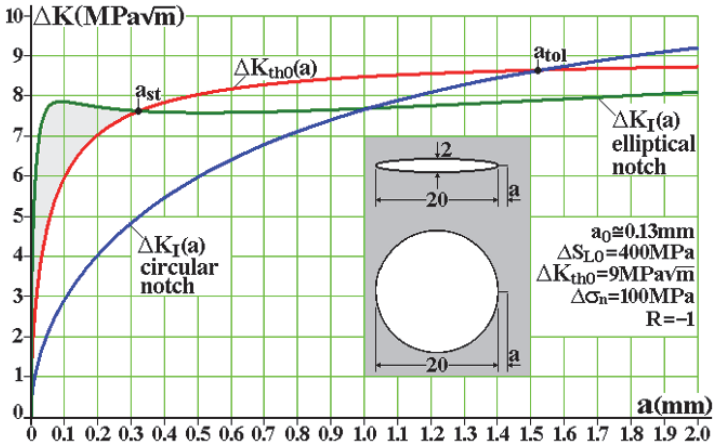

Figure 1: According to the short crack model, cracks should not initiate at the circular hole (which tolerates cracks $a_{tol} < 1.52mm$), while the crack that initiates at the elliptical hole tip should stop at $a_{st} \cong 0.33mm$.

It is interesting to emphasize the practical usefulness of modeling the short crack behavior in notched components. The classic *SN* and εN methodologies are very much used to analyze and to design supposedly crack-free structural components in engineering applications, even though it is impossible to guarantee that they are really free of cracks smaller than the guaranteed detection threshold of the non-destructive inspection method used to identify them. In fact, although large cracks may be detected and dealt with in practice, microcracks and mechanically short cracks are practically undetectable by traditional non-destructive inspection methods. Nevertheless, most components are still designed against fatigue crack initiation using procedures that do not recognize such unavoidable small flaws. So, their service life expectancy may become unreliable when such tiny defects are introduced by any means during manufacturing or service.

Therefore, structural components that must last for long fatigue lives should be designed not only to avoid crack initiation, but also to be tolerant to undetectable short cracks. Indeed, continuous work under fatigue loads cannot be guaranteed if any of the flaws that they might have (because they could not be or have not been detected) can somehow propagate during their service lives. However, despite self-evident, this prudent requirement is still not included in most *SN* and εN fatigue design routines used in practice. Indeed, most long-life designs just intend to maintain the service stresses at the structural component's critical point below its fatigue limit, $\Delta\sigma < \Delta S_{LR}/\phi_F$, where ϕ_F is a suitable safety factor for fatigue applications. So, although such calculations can be quite complex (e.g. when analyzing fatigue crack initiation caused by random multiaxial non-proportional loads), their so-called *safe-life* philosophy is not that safe.

However, despite neglecting the effect of any cracks or crack-like defects, most long-life fatigue designs do work quite well in practice. This means that they are somehow tolerant to undetectable or to functionally-admissible short cracks. Nevertheless, the question "how much tolerant" cannot be answered by *SN* and εN procedures alone. This potentially important problem can be dealt with by adding short crack concepts to their infinite life design criteria, which may be given (in its simplest version) by

$$\Delta\sigma < \Delta K_{thR} \Big/ \left\{ \phi_F \cdot \sqrt{\pi a} \cdot g(a/w) \cdot \left[1 + (a_R/a)^{\gamma/2} \right]^{1/\gamma} \right\}, \; a_R = (1/\pi) \cdot (\Delta K_{thR} / \eta \Delta S_{L\text{-}R})^2 \tag{4}$$

Since the fatigue limit ΔS_{LR} at a given fixed $\{\Delta\sigma, R\}$ condition already reflects the effect of microstructural defects inherent to the material, Eq. (4) complements it by describing the tolerance to small cracks that may go unnoticed in actual service conditions.

A practical example can illustrate well how these ideas can be useful in engineering applications. Due to a rare manufacturing problem, a batch of a small but important structural component was delivered with tiny scratch-like elongated surface cracks only detectable by under a microscope, causing some serious unexpected failures when mounted in the machine it usually worked forever. The question is how to estimate the effect of such small crack-like defects in the fatigue strength of those components, knowing that each piece has a 2 by 3.4mm rectangular cross-section and is made of a steel with ultimate strength $S_U = 990MPa$ and (uncracked) fatigue limit $S_L = 246MPa$.

The piece fatigue limit is about $S_U/4$, whereas steels typically have $S_L \cong S_U/2 = 495MPa$. This difference may be due to a surface finish factor $k_{sf} \cong 0.5$, a value between those proposed by Juvinall for $S_U \cong 1GPa$ steels with cold-drawn or machined surfaces, $0.45 \le k_{sf} \le 0.7$ [10]. Although surface finish should not affect the growth of fatigue cracks, the measured value could be due to other factors as well, like e.g. tensile residual stresses near the piece surface. Hence, the only safe option is to use $S_L = 246MPa$ to evaluate the short crack effects, estimating the fatigue limit at $R > -1$ (or at $\sigma_m > 0$) e.g. by Goodman as $S_L(R) \equiv S_{LR} = S_L S_U(1-R)/[S_U(1-R) + S_L(1+R)]$.

The FCG threshold is also needed to model short crack effects. If data is not available, as in this case, it must be estimated e.g. by $\Delta K_{th}(R \le 0.17) \cong \Delta K_{th0} = 6MPa\sqrt{m}$ and $\Delta K_{thR}(R > 0.17) = 7 \cdot (1 - 0.85R)$ [3]. This risky practice increases the prediction uncertainty, but it was the only option available. However, this estimate is conservative regarding typical data, which tend to indicate $6 < \Delta K_{th0} < 12MPa\sqrt{m}$. Moreover, it assumes $\Delta K_{thR}(R < 0) \cong \Delta K_{th0}$, usually a safe estimate as well (unless the load history contains severe compressive underloads that may accelerate the crack, not the case here). Using the SIF of an edge-cracked strip of width **w** loaded in mode I [3], Fig. 2 shows the tolerable stress ranges under pulsating axial loads estimated within a fatigue safety factor ϕ_F by:

$$\Delta\sigma_0 \le \frac{\Delta K_{th_0} \Big/ \left(\phi_F \sqrt{\pi a} \right)}{\sec\frac{\pi a}{2w} \sqrt{\frac{2w}{\pi a} \tan\frac{\pi a}{2w}} \left[0.752 + 2.02\frac{a}{w} + 0.37\left(1 - \sin\frac{\pi a}{2w} \right)^3 \right] \left[1 + \left(\frac{a_0}{a} \right)^{\gamma/2} \right]^{1/\gamma}} \tag{5}$$

This simple (but quite reasonable) model indicates that the studied structural component tolerates well small edge cracks up to $a \cong 30mm$, which almost do not affect its original fatigue limits. However, since this conclusion is based on estimated properties, Fig. 3 evaluates the influence of the threshold ΔK_{th0} and of the data-fitting exponent γ on the values estimated for the tolerable stress ranges, enhancing how important it is to measure them to obtain less-scattered predictions. Nevertheless, in spite of this scatter, such estimates can be very useful for designers and quality control engineers. They can be used e.g. as a quantitative tool if a production or an operational accident damages the surface of otherwise well-behaved components, to help deciding whether they can be kept in service or must be recalled.

These estimates provide interesting results, but they have some intrinsic limitations. They assume the short crack grows unidimensionally, thus can be characterized by its size *a* only, when surface flaws much smaller than the piece dimensions probably look like small surface or corner cracks, and should be treated as so. 2D cracks grow by fatigue in two directions, usually changing their shape at every load cycle, although maintaining their original plane under mode I loads, see [3]. In fact, cracks (short or long) should not be modeled as 1D unless their fronts uniformly cut the whole piece thickness and can be described by just 1 coordinate. Moreover, these estimates are only valid for mechanically short cracks, those with both *a* and a_0 larger than the grain size of the material *gr*. The FCG behavior of microcracks with sizes *a* and $a_0 < gr$ is

sensitive to microstructural features, but since grains (let alone dislocations) cannot be mapped in practical applications yet, their use for structural engineering purposes may be questionable.

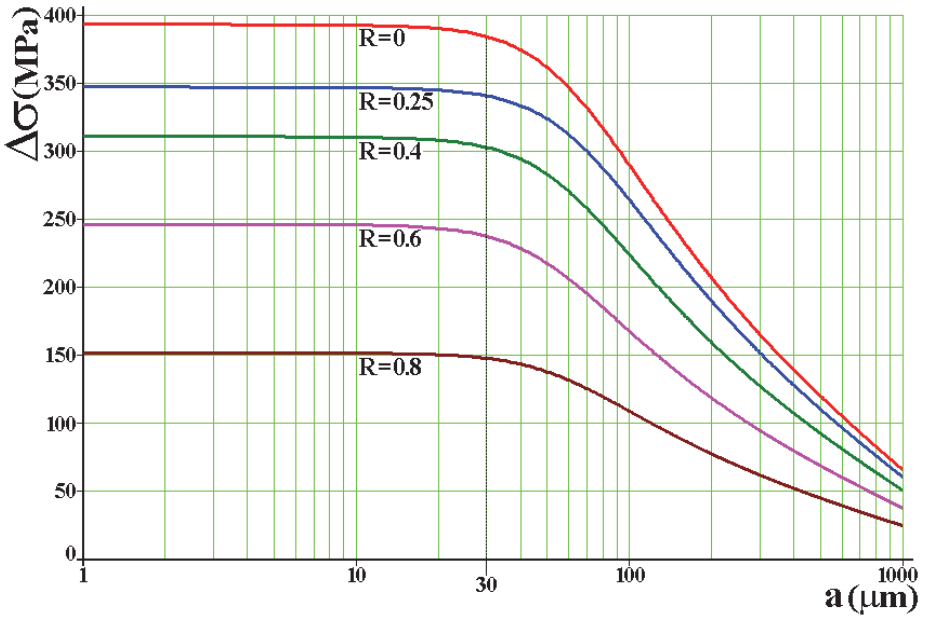

Figure 2: Larger stress ranges $\Delta\sigma$ tolerable by the studied component under many R–ratios as a function of the size a of an edge crack, for $w = 3.4mm$, $h = 1.12$, $\Delta K_{th0} = 6MPa\sqrt{m}$, $a_0 = 59mm$, $\gamma = 6$, and $\phi_F = 1.6$.

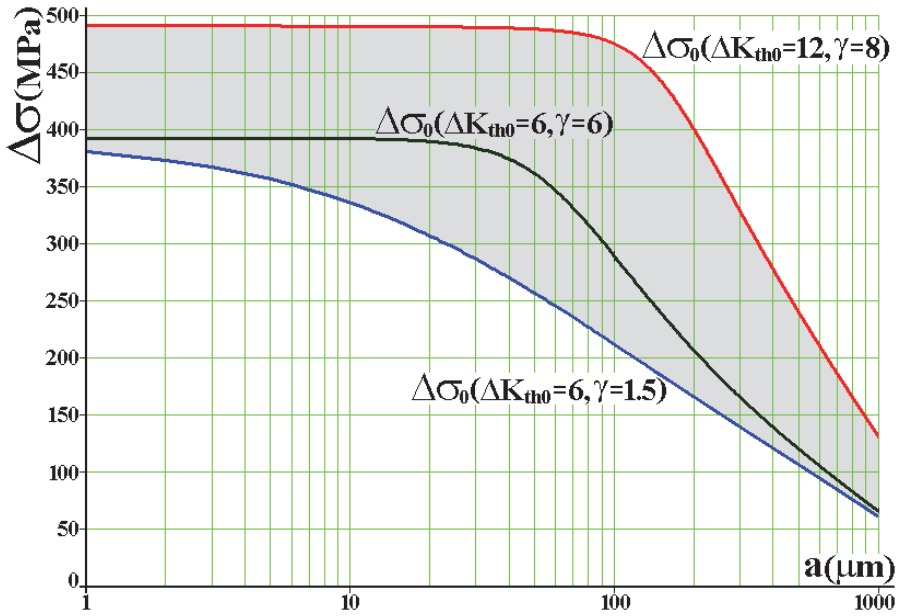

Figure 3: Influence of the typical ranges of FCG threshold $6 < \Delta K_{th0} < 12MPa\sqrt{m}$ and of Bazant's data-fitting exponent $1.5 < \gamma < 8$ on the largest stress ranges $\Delta\sigma_0$ tolerated by the studied piece.

THE BEHAVIOR OF SHORT CRACKS UNDER EP CONDITIONS

Under contained elastoplastic conditions around crack tips, which invalidate the use of SIFs to quantify the local crack driving forces, the non-propagating crack problem can be modeled using the J-integral approach [13-14], as originally proposed in [7]. However, since like in the LE case short fatigue cracks present higher FCG rates than

long cracks in the EP case as well, it is operationally convenient to modify their $J_{th}(a)$ propagation threshold to consider the effects of the short crack characteristic size a_0 when accounting for their peculiar behavior near EP notch tips. In the LE case, the size-dependent threshold $J_{th}(a)$ must of course be given by $K_{th}(a)/E'$, where $E' = E$ or $E' = E/(1 - \nu^2)$ for plane stress or plane strain limit conditions. In this way, $J_{th}(a)$ can then be easily compared with the crack driving force quantified by J when modeling the EP short crack behavior.
If the stresses controlled by J grow proportionally to the load P applied on the cracked piece, then for a Ramberg-Osgood material with strain-hardening coefficient H and exponent h, it can be shown [3] that the crack driving force J is given in clear engineering notation by:

$$J = J_{el} + J_{pl} = K_I^2/E' + \left[\left(P/P_{pc}\right)S_Y\right]^{(1+h)/h}\left[(w-a)/H^{1/h}\right]\mathrm{h}(a/w,h) \tag{4}$$

where $K_I(P)$ is the SIF applied on the cracked piece (as if it remained LE), P_{pc} is the plastic collapse load, S_Y is the yielding strength, w is the cracked piece width, $w - a$ is its residual ligament, and h is a non-dimensional function that depends on the cracked piece geometry and on the strain-hardening exponent. Although not as easy to find as K_I values, h-values may be found in tables for some simple geometries. However, this is not a major barrier in practice, since they can nowadays be calculated in most finite element (FE) codes for more complex components. To model the short crack behavior, like its LE analog $K_{th}(a)$, the size-dependent crack propagation threshold $J_{th}(a)$ must include the a_0 effect:

$$J_{th}(a) = J_{th}/(1 + a_0/a) \tag{5}$$

Hence, like in the LE case, EP cracks grow whenever their driving force J is higher than their size-dependent threshold J_{th}(a), a material property that can be properly measured, and stop otherwise. Cracks that depart from a notch tip can be much affected by the notch stress gradient when their size is small or similar to the notch tip radius ρ, so they can start and then stop after growing for a while, becoming thus non-propagating. Figure 4 e.g. shows J for a crack that departs from a notch with $\rho = 1mm$ and stops at a size $a = 1.8mm$, when its J become smaller than its threshold $J_{th}(a)$, becoming non-propagating. If P remains fixed, notice that this cracked component would then tolerate cracks with size $1.8 < a < 9mm$.

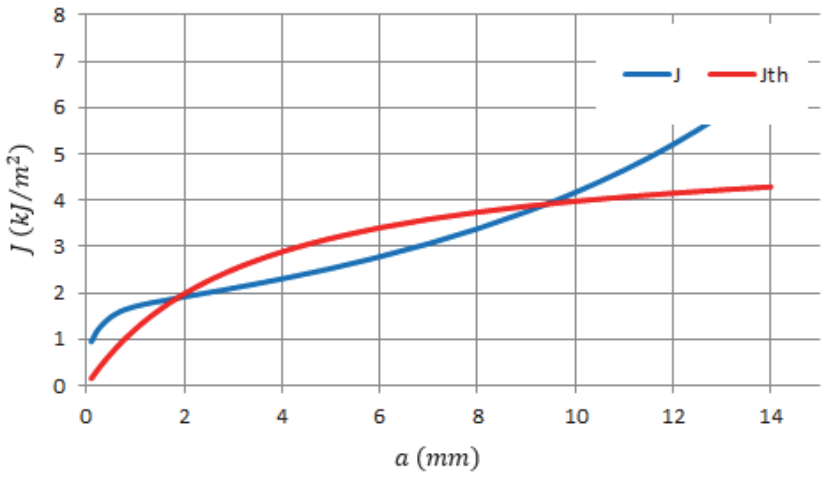

Figure 4: EP crack that starts at a notch tip and then stops after growing for 1.8mm.

EXPERIMENTAL EAC RESULTS

Curves $K_I(a)\times a$ and $J_I(a)\times a$ are generated for notched DC(T) specimens by repeated finite element analyses performed using a suitable 2D Abaqus/CAE FE model, considering EP conditions near the notch tip as needed. These curves, which quantify the crack driving force, can be compared with the $K_{EACth}(a)\times a$ and $J_{EACth}(a)\times a$ curves, which quantify the material resistance to EAC conditions, including the short crack effects. These comparisons are very

helpful in practice, since they can visually map the whole cracking problem. This visual technique is then used to make predictions about the short crack behavior that can be experimentally verified. To do so, notched DC(T)s of AISI 4140 steel (whose crack initiation and long crack growth EAC thresholds in a solution of H_2S, $S_{EAC} = 332MPa$ and $K_{EACth} = 34.2MPa\sqrt{m}$, have been previously measured by ASTM F1624 and ISO 7539 standards, and by NACE procedures [10]) are tested under EAC conditions as follows.

First, two DC(T)s with a useful width $w = 60mm$ and a notch of length $b = 15mm$ and tip radius $\rho = 2mm$ are EAC tested in the H_2S solution under two load levels, $P = 6750N$ and $P = 8250N$, which induce LE conditions around the notch tip. According to the short crack models presented above, the first should generate a non-propagating crack, see Fig. 5, whereas the second should start and propagate a crack, see Fig. 6, as indeed they did, see Fig. 7.

In the sequence, two other similar DC(T) specimens, one with notch tip radius $\rho = 0.2mm$ and loaded by $P = 3.1kN$ and the other with $\rho = 0.3mm$ and loaded by $P = 6kN$, were EAC tested in the same aggressive environment, but now under EP conditions around the notch tip. Considering their size-dependent threshold $J_{th}(a)$ and their crack driving forces J, both specimens should withstand the loads without breaking, as indeed they did, see Fig. 8-10.

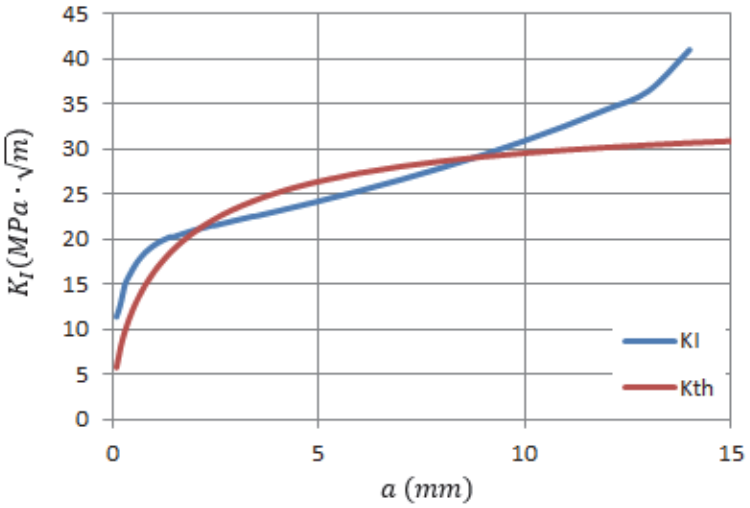

Figure 5: Curves $K_I(a) \times a$ and $K_{EACth}(a) \times a$ generated by the analysis of the linear elastic DC(T) under EAC and $P = 6750N$.

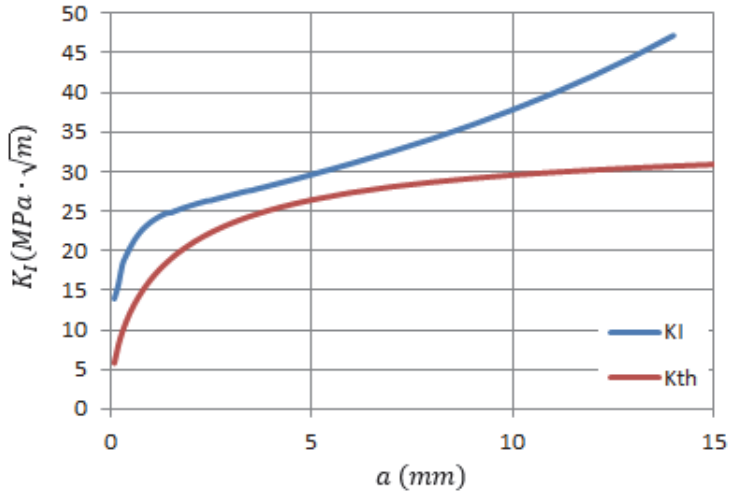

Figure 6: Curves $K_I(a) \times a$ and $K_{EACth}(a) \times a$ generated by the analysis of the linear elastic DC(T) under EAC and $P = 8250N$.

Figure 7: LE specimens after working 30 days under EAC conditions in an aqueous hydrogen sulfide environment.

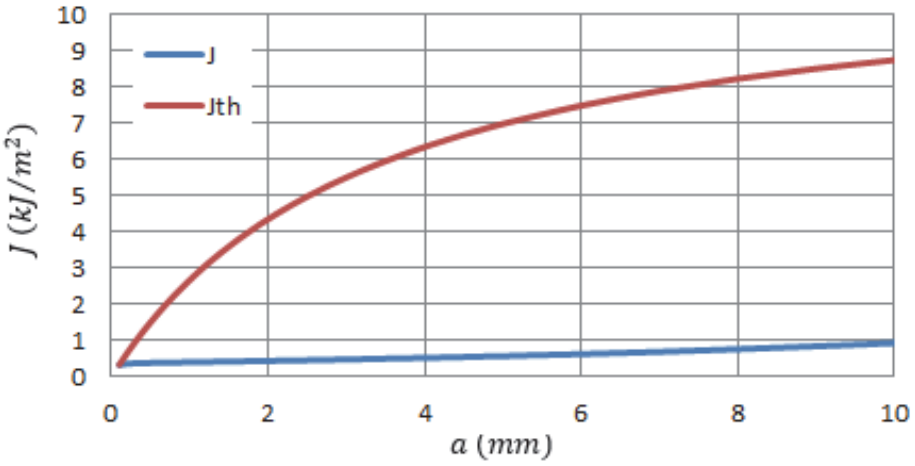

Figure 8: Curves $J_I(a)\times a$ and $J_{EACb}(a)\times a$ generated by the analysis of the DC(T) loaded by $P = 3.1kN$ under EP conditions.

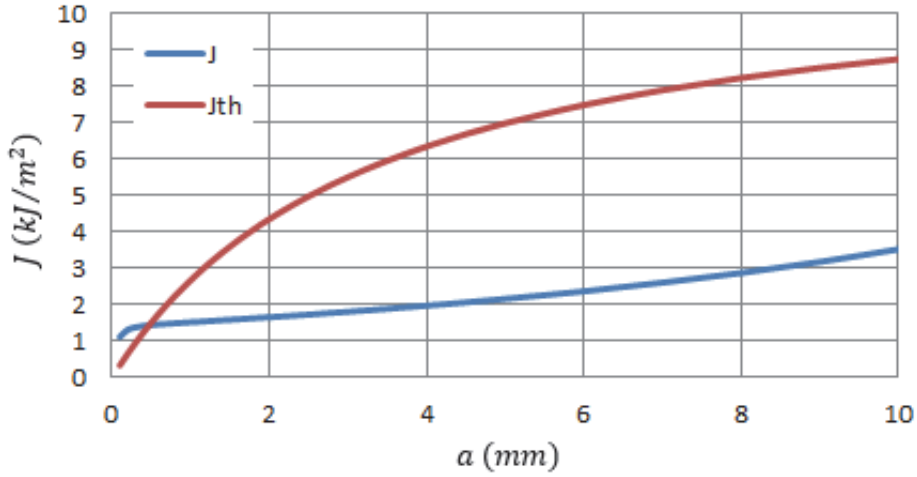

Figure 9: Curves $J_I(a)\times a$ and $J_{EACb}(a)\times a$ generated by the analysis of the DC(T) loaded by $P = 6kN$ under EP conditions.

Figure 10: EP specimens after 30 days under EAC in aqueous hydrogen sulfide environment.

CONCLUSIONS

The proposed model is able to evaluate the propagating or non-propagating behavior of short cracks that depart from notch tips under linear elastic and elastic-plastic load regimes for any geometry and applied load. Hence, it can be used to assess the size of tolerable short cracks or crack-like defects in practical applications. This work presents experimental evidence to support this claim under stress corrosion cracking conditions, but a similar mechanics is also valid for modeling the behavior of short fatigue cracks.

REFERENCES

[1] Frost, N.E., Marsh, K.J., Pook, L.P., Metal Fatigue, Dover (1999).
[2] Taylor, D., The Theory of Critical Distances, Elsevier (2007).
[3] Castro, J.T.P., Meggiolaro, M.A., Fatigue Design Techniques, volume 3: Crack Propagation, Temperature and Statistical Effects. CreateSpace (2016).
[4] Castro, J.T.P., Meggiolaro, M.A., Miranda, A.C.O., Wu, H., Imad, A., Nouredine, B., Prediction of fatigue crack initiation lives at elongated notch roots using short crack concepts, Int J Fatigue, 42 (2012) 172-182.
[5] Castro, J.T.P., Landim, R.V., Leite, J.C.C., Meggiolaro, M.A., Prediction of notch sensitivity effects in fatigue and EAC., Fatigue Fract Eng Mater Struct, 38 (2015) 161-179.
[6] Castro, J.T.P., Landim, R.V., Meggiolaro, M.A., Defect tolerance under environmentally-assisted cracking conditions. Corrosion Reviews, 33 (2015) 417-432.
[7] El Haddad, M.H., Topper, T.H., Smith, K.N., Prediction of non-propagating cracks. Eng Fract Mech, 11 (1979) 573-584.
[8] El Haddad, M.H., J-integral applications for short fatigue cracks at notches, Int J Fract,16 (1980) 15-30.
[9] Shigley, J.E., Mischke, C.R., Budynas, R.G., Mechanical Engineering Design, 7th ed., McGraw-Hill (2004).
[10] Juvinall, R.C., Marshek, K.M., Fundamentals of Machine Component Design, 4th ed., Wiley (2005).
[11] Norton, R.L., Machine Design, An Integrated Approach, 3rd ed., Prentice-Hall (2005).
[12] Peterson, R.E., Stress Concentration Factors, Wiley (1974).
[13] Shih, C.F., Hutchinson, J.W., Fully Plastic Solutions and Large Scale Yielding Estimates for Plane Stress Crack Problems, J Eng Mater Technology, 98 (1976) 289-295.
[14] Goldman, N.L., Hutchinson, J.W.m Fully Plastic Crack Problems: the center-cracks strip under plane strain. Int J Solids Struct, 11 (1975) 575-591.
[15] ASTM E-1820-13: Standard test Method for Measurement of Fracture Toughness. ASTM (2014).
[16] NACE TM0177: Laboratory Testing of Metals for Resistance to Sulfide Stress Cracking and Stress Corrosion Cracking in H_2S Environments. NACE (2005).